CONF-900918--6

UCRL-JC--104573

DE91 000286

# ECH by FEL and Gyrotron Sources on the MTX Tokamak

B. W. Stallard, W. C. Turner, S. L. Allen, J. A. Byers, B. Felker,
M. E. Fenstermacher, S. W. Ferguson, E. G. Hooper,
M. A. Makowski, K. I. Thomassen, and A. L. Throop



This paper was prepared for submittal to
Proc. 16th Symposium on Fusion Technology
London, U.K., September 3–7, 1990

August 9, 1990

Lawrence Livermore National Laboratory

## DISCLAIMER

# ECH BY FEL AND GYROTRON SOURCES ON THE MTX TOKAMAK*

B. W. Stallard, W. C. Turner, S. L. Allen, J. A. Byers, B. Felker, M. E. Fenstermacher,
S. W. Ferguson, E. G. Hooper, K. I. Thomassen, and A. L. Throop (LLNL)
M. A. Makowski (TRW, Inc., Redondo Beach, CA)

## ABSTRACT

The Microwave Tokamak Experiment (MTX) at LLNL is studying the physics of intense pulse ECH in a high-density tokamak plasma using a microwave FEL. Related technology development includes the FEL, a windowless quasi-optical transmission system, and other microwave components. Initial plasma experiments have been carried out at 140 GHz with single rf pulses generated using the ETA-II accelerator and the ELF wiggler. Peak power levels up to 0.2 GW and pulse durations up to 10 ns were achieved for injection into the plasma using an untapered wiggler. FEL pulses were transmitted over 33 m from the FEL to MTX using six mirrors mounted in a 50-cm-diam evacuated pipe. Measurements of the microwave beam and transmission through the plasma were carried out. For future rapid pulse experiments at high average power (4 GW peak power, 5 kHz pulse rate, and $\overline{P} > 0.5$ MW) using the IMP wiggler with tapered magnetic field, a gyrotron (140 GHz, 400 kW cw or up to 1 MW short pulse) is being installed to drive the FEL input or to directly heat the tokamak plasma at full gyrotron power. Quasi-optic techniques will be used to couple the gyrotron power. For direct plasma heating, the gyrotron will couple into the existing mirror transport system. Using both sources of rf generation, experiments are planned to investigate intense pulse absorption and tokamak physics, such as the ECH of a pellet-fueled plasma and plasma control using localized heating.

*Work performed by LLNL for USDOE under contract W-7405 ENG-48.

## 1. INTRODUCTION

The main physics objective for the MTX experiment is the study of intense pulse ECH in a high-density tokamak[1] plasma using a microwave FEL. For these experiments, technology development is required for both the FEL and a transmission system to transport the FEL power to the tokamak. In this paper we report our initial experiments at 140 GHz with single rf pulses generated using the ETA-II induction linac[2] and the ELF-II wiggler.[3]

We are also preparing for future multiple pulse experiments at high average power using the Intense Microwave Prototype (IMP) wiggler with a tapered magnetic field. A gyrotron is being installed to drive the FEL input or to directly heat the tokamak plasma. Both Vlasov-type antennas and a new device, MAGICTRAC, will be used to couple the gyrotron power. For direct plasma heating, the gyrotron couples into the existing mirror transport system.

## 2. FEL OPERATIONS

For the single pulse experiments, the ELF-II wiggler (9.8 cm wiggler wavelength, 4 m total length, and 0.5 Hz repetition rate for the pulsed wiggler magnets) was used.[3] The e-beam parameters produced by the ETA-II accelerator were 6 MeV, 2 kA, and 50 ns pulse length. The dominant waveguide mode for interaction with the e-beam was $TE_{01}$ in WR229 waveguide (5.82 x 2.91 cm). For nontapered operation of the wiggler, peak power levels up to 0.2 GW and pulse widths up to 10 ns were achieved at 140 GHz. Figure 1 shows an experimental gain curve for the wiggler, obtained by varying the length of energized magnets. The input drive power was 20 W from an EIO source, injected into the wiggler waveguide co-linear with the e-beam. At the available drive power and beam current, the FEL interaction just reached saturation.

The rf pulse length was limited by spatial and energy sweep in the output beam of the linac. Energy sweep affected the synchronism of the e-beam and the interacting waveguide modes. Energy sweep, combined with imperfect magnetic alignment of transport magnets in the linac, also caused a "corkscrew" motion, or spatial sweeping, of the e-beam in the transverse plane.[4] These displacements of the beam from the waveguide axis reduced the FEL interaction, the pulse reproducibility, and the power output.

Because of the low input drive power and the corkscrew motion, it was not possible to achieve strongly tapered operation. With these limitations, a preliminary attempt at tapering the wiggler produced pulses up to 0.4 GW.

## 3. BEAM TRANSPORT AND MTX INJECTION

The FEL pulse was injected into the windowless, quasi-optical transport system (Fig. 2), which consists of 6 aluminum mirrors within an evacuated stainless steel pipe of 50 cm diameter. The total transport distance to MTX is 33.3 m. The mirror optics were designed using the MTH code,[5] which calculates transport by solution of Huygens' equation. For the $TE_{01}$ mode, the calculated transport efficiency is 89%; the calculated profiles at several points in the system are shown in Fig. 3. Most of the transport loss arises from spillage of side-lobe power at the first three optics. The resulting beam profile at MTX is nearly Gaussian and elongated vertically in the H-plane.

Measurements of an FEL pulse at the input and output of the transport system and the horizontal beam profile near the input to MTX are shown in Fig. 4. The measurements in Fig. 4 a and b are single-point measurements at the mirror centers of $J_0$ and $M_4$, respectively, made using a calibrated Shottky diode receiver. Calibration uncertainties were ±2 dB. Because the measurement is single point and because computer simulation of the FEL interaction for nontapered operation predicts multimode output, an accurate determination of transmission efficiency has not been made. This awaits future measurement using total-beam calorimetry.

The plotted points for the profile in Fig. 4c, measured 1.23 m downstream from $M_4$ using a movable detector, are six-pulse averages at each measurement point. Also plotted is the calculated profile for transport of the $TE_{01}$ mode. Differences between the measured and calculated profiles can arise from (a) interference between several modes generated by the FEL and (b) interference between the beam and scattering from the detector probe. The dominant mode competing with $TE_{01}$ is predicted to be $TE_{21}$. This mode has a poor transmission efficiency (~37%), so only a small fraction of the total power would appear in the undesired mode.

The transmission loss is low only for those modes that propagate from mirror to mirror. For a pulse with 55 MW peak power, Fig. 5 shows late pulse "rattle" at MTX of side-lobe power from the $TE_{01}$ and non-$TE_{01}$ modes, which are transit-time delayed from the main beam pulse. Power that misses the mirrors reflects from the lossy stainless steel walls of the vacuum pipe. Because of 90 deg bends in the beam line, the side-lobe power propagates at large angles to the system axis, and many wall reflections are required for transport to MTX, resulting in large attenuation and longer transit time. The dashed curve in the figure is the decay rate for a model with a reflection loss $\eta \approx 0.02$. From this we infer a 3-fold enhancement in the reflection loss calculated from the dc measured resistivity.

Single point measurements of transmission through plasma discharges at the beam center are shown in Fig. 6 for the resonance located on the toroidal axis ($B_t = 5$ T). Also plotted are curves from ray tracing calculations showing the attenuation due to plasma refraction alone and the attenuation with absorption included.[6] For the calculations, the model profiles $n_e/n_0$, $T_e/T_{e0} \sim [1-(r/a)^2]^\alpha$ are used, where $\alpha = \alpha_n$ or $\alpha_T$ for density and temperature, respectively. The shaded areas show the dependences of refraction and absorption that bound the shot-to-shot changes in the measured profiles of electron temperature and density. Data for both low power (~1 W for EIO driver power only) and high power with the FEL are shown. Within large measurement uncertainties, the transmission is power independent, which indicates no departure at these power levels from linear absorption, in agreement with expectations.

The data show a strong decrease with plasma density and fall within the bounds calculated for absorption. The large error bars in transmission with the EIO alone result from large variations during the 5 $\mu$s EIO pulse. We postulate that scattering from density fluctuations and interference at the single point detector, from multipath transmission of power through the plasma, may play a role.

## 4. GYROTRON COUPLING

For the next phase of experiments, the IMP wiggler[7] will be used. The wiggler magnets operate cw, and experiments with a 50-pulse burst at 5 kHz are planned with peak and average power levels of 4 GW and >0.5 MW, respectively. The wiggler drive power will be greatly increased by use of a 400 kW, 140 GHz gyrotron, which will be coupled into the wiggler input by the system shown in Fig. 2. Gyrotron power in the $TE_{15,2}$ mode is converted to a directive beam with a Vlasov-type antenna,[8] which in turn is focused into the wiggler input. The rf beam is coupled co-linearly to the e-beam after reflection from a mirror with a central hole for passage of the e-beam.

Alternatively, we can directly heat the tokamak plasma by coupling the gyrotron power into the existing transport system, also shown in Fig. 2. Initial coupling to the transmission system will use a Vlasov-type converter. We also will test coupling of a new device, MAGICTRAC,[9] shown in Fig. 7. MAGICTRAC consists of a mode-converting taper and three optics. The taper converts the $TE_{15,2}$ gyrotron to a mode mixture of $TE_{15,2}$ and $TE_{15,3}$, which has zero wall electric fields at the end of the taper. Mirror $M_1$ incorporates steps and a tilt in the mirror surface, which is shaped like a counterbore tool bit, to convert skew rays ($k_\phi \neq 0$) of the incident microwave power into nonskew rays. $M_2$ has twist reflector grooves in the surface to linearly polarize reflected fields, and $M_3$ corrects the phase of the annular converging beam from $M_2$ to produce a Gaussian-like output beam.

Figure 8 shows the calculated aperture field on $M_3$, where the phase fronts of the reflected beam are nearly planar, and Fig. 9 shows the beam profile at a distance of 8 m. The beam is highly symmetric, and the cross-polarized power is <1%. The calculated fraction of power within the main lobe exceeds 96%. Higher efficiency may be possible by further optimization.

## 5. PLASMA EXPERIMENTS

Using both sources of rf generation, we can compare intense pulse absorption for the FEL with linear absorption of gyrotron power. A pellet injector capable of 4-pellet injection is operational on MTX, and heating of peaked-density-profile plasmas, fueled by pellet injection, will be carried out. Important issues are confinement and transport in such profiles. We also are planning experiments to control MHD modes by the localized absorption of ECH power. The growth of low-order tearing modes (poloidal mode numbers $m = 2$ and 3) is believed to cause plasma disruptions. Such modes have been identified in MTX with frequencies in the 8–18 kHz range. The rf systems are capable of modulation of heating power at the fundamental (for the gyrotron) or a subharmonic frequency (for the FEL), with phase-controlled feedback, to investigate MHD control.

## 6. CONCLUSIONS AND FUTURE UPGRADES

Initial operations have verified nontapered operation of the FEL at 140 GHz and the design of the quasi-optic transport system. Diagnostics with nanosecond response have been developed for measurements of FEL pulses. ETA-II has recently undergone several modifications to increase the FEL output pulse from 10 to 35 ns and to provide for burst mode operation at 5 kHz. These modifications include improvements in the pulse distribution system to the accelerator cells[10] and in the magnetic alignment of the solenoids used to focus the e-beam.[11] The new pulse distribution system will increase the duration of the ±1% energy flattop to 35 ns. These improvements are expected to reduce spatial sweeping of the e-beam at the accelerator exit from $\pm 1$ cm to less than $\pm 1$ mm.[12] With greater input drive power and installation of the IMP wiggler, tapered operation of the wiggler is expected to increase peak power so that the physics of intense pulse heating can be addressed.

REFERENCES


1. W. M. Nevins et al., *Phys. Rev. Lett.* **59** (1987) 60.
2. J. C. Clark et al., *1988 Linear Accel. Conf. Proc.*, Williamsburg, VA, **19** (1988).
3. A. L. Throop et al., *Proc. 11th Int. Conf. Free Elec. Lasers*, Naples, FL (1989).
4. W. E. Nexsen et al., *ibid.*
5. T. Samec, *Bull. Am. Phys. Soc.* **32** (1987) 1872.
6. G. Smith et al., Modeling of Electron-Cyclotron Power Profiles on a Calorimeter in the Microwave Tokamak Experiment, UCRL-JC-103455 (1990); submitted to *Nucl. Fusion*.
7. R. A. Jong et al., *Nucl. Instr. and Methods in Phys. Res.* **A285** (1989) 379.
8. S. N. Vlasov et al., *Radio Eng. Electron. Phys.* **20** (1975) 14.
9. B. W. Stallard et al., *Int. J. Infrared and Millimeter Waves* **9** (1990).
10. S. Sampayan et al., *Proc. 1990 Linear Accel.Conf.*, Albuquerque, NM (1990).
11. L. V. Griffith et al., *ibid.*
12. W. C. Turner et al., *ibid.*

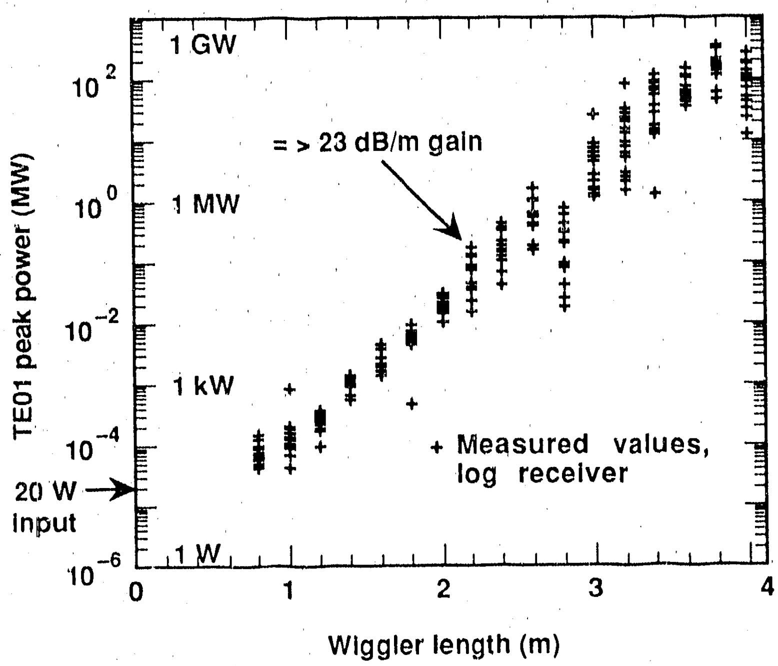


FIGURE 1. Measured gain curve for nontapered operation at 139.5 GHz. Beam parameters are 5.8 MeV and 1.6 kA.

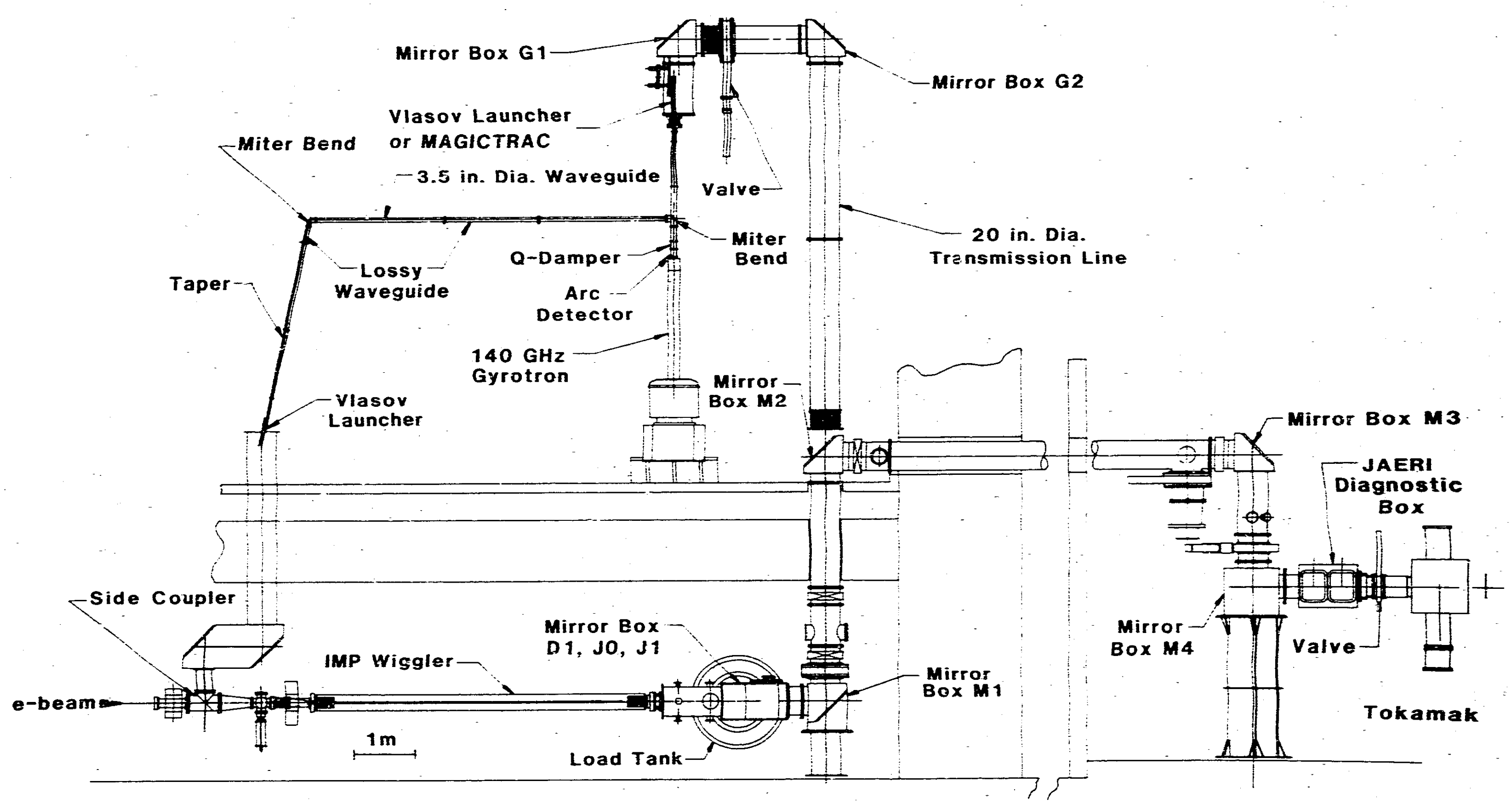


FIGURE 2. Drawing of the MTX microwave system showing the input and output coupling to the FEL and gyrotron and the quasi-optic transport system to MTX

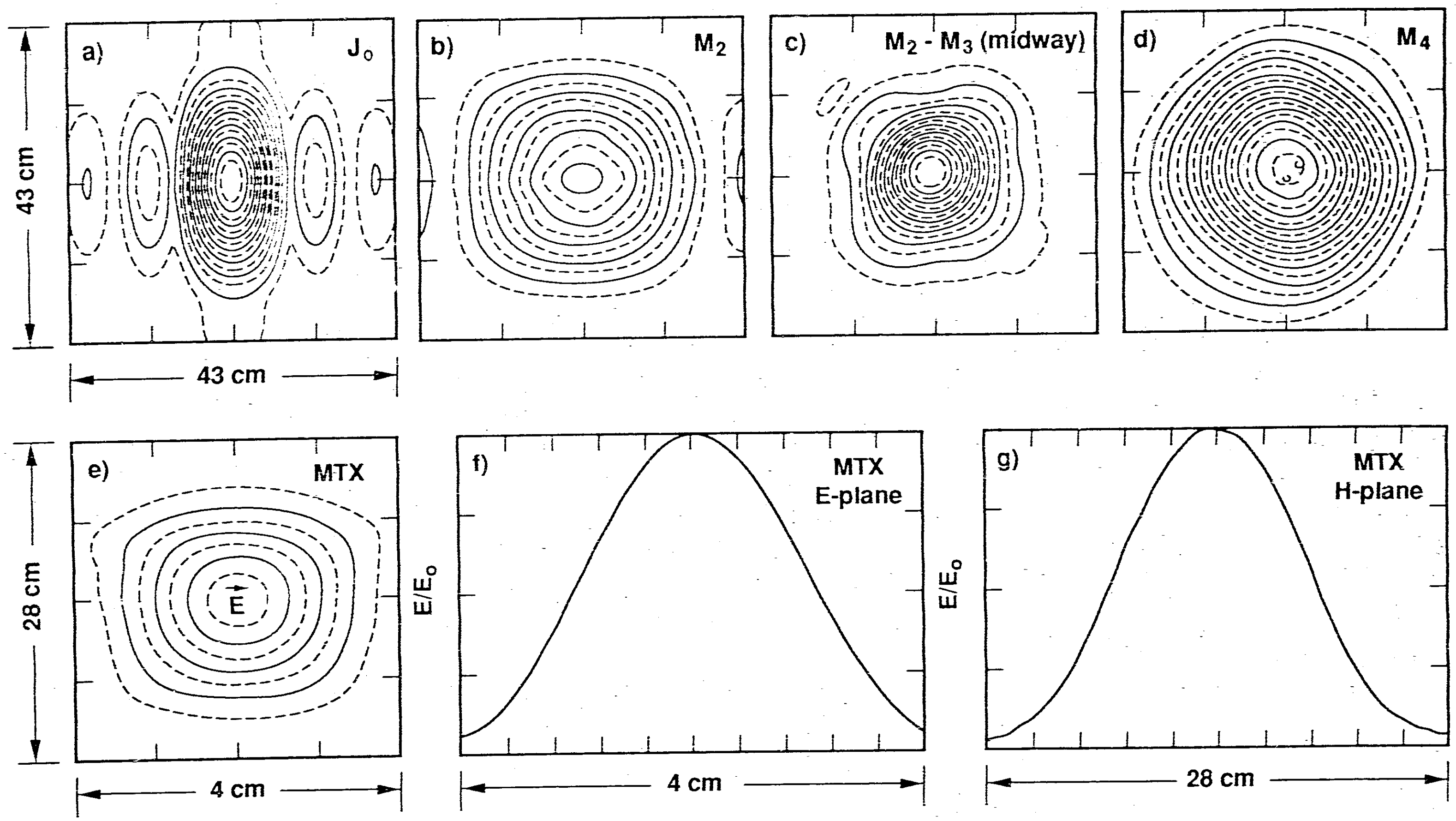


FIGURE 3. Computed microwave beam profiles for the $TE_{01}$ mode at several mirror optics and at the MTX port.

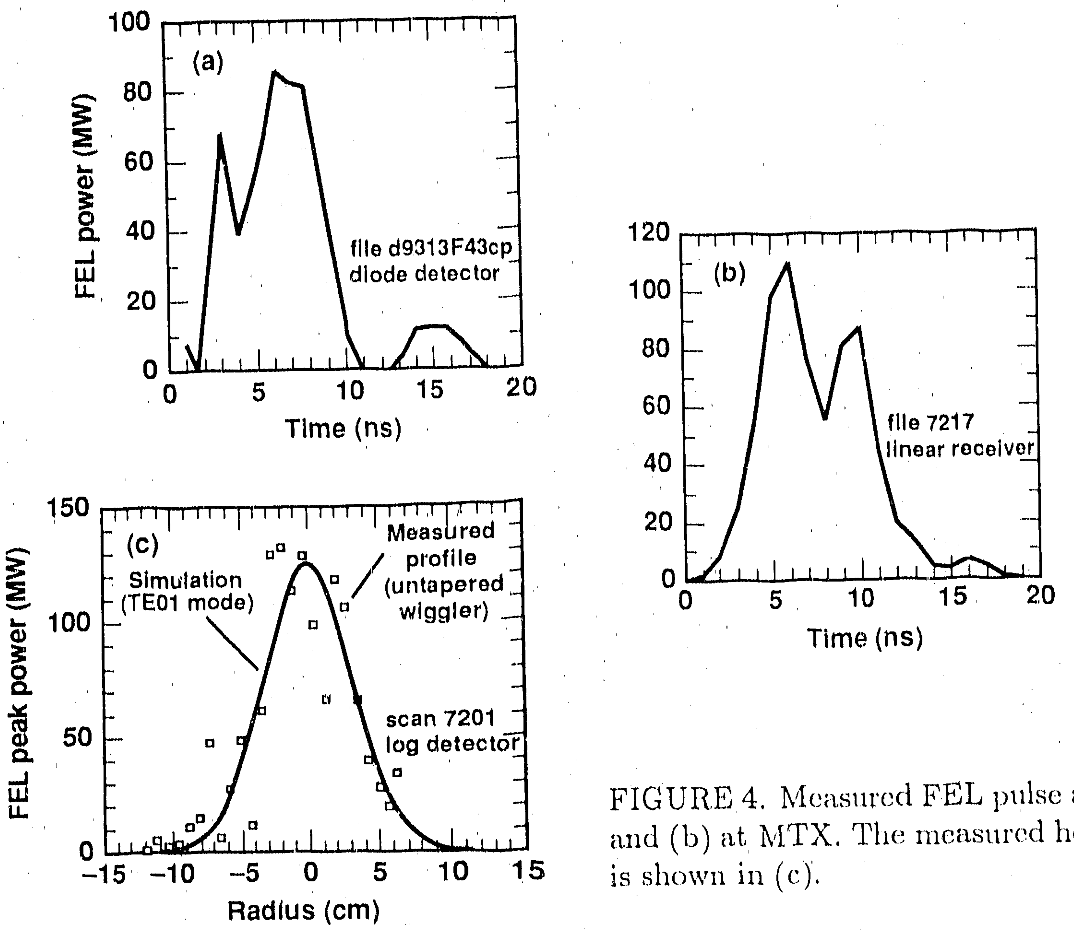


FIGURE 4. Measured FEL pulse at (a) the FEL output and (b) at MTX. The measured horizontal beam profile is shown in (c).

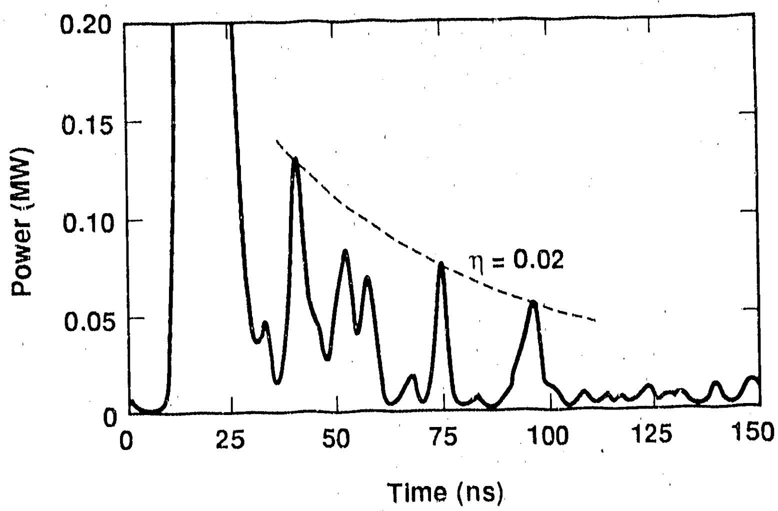


FIGURE 5. Late pulse "rattle" for side-lobe power, following a main pulse of 55 MW peak power.

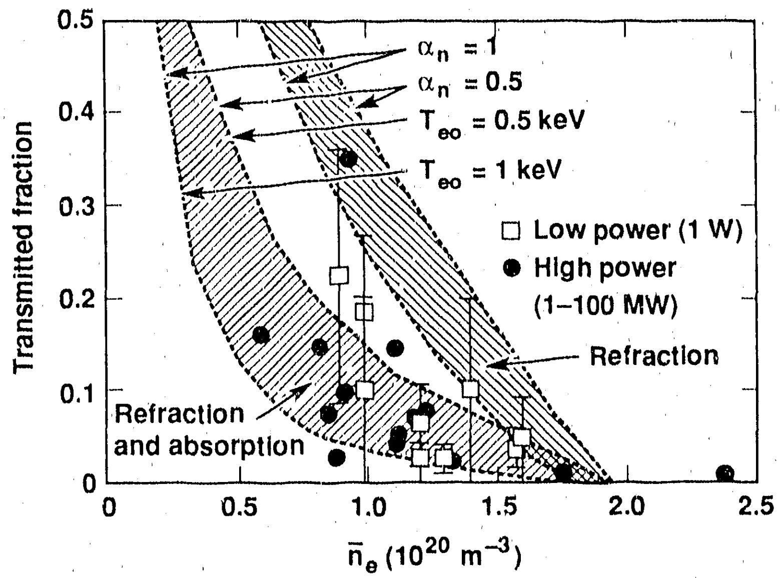


FIGURE 6. Measured plasma transmission for FEL and EIO power for central resonance. Profile parameter $\alpha$ is defined in the text. For the electron profile $\alpha_T = 1$.

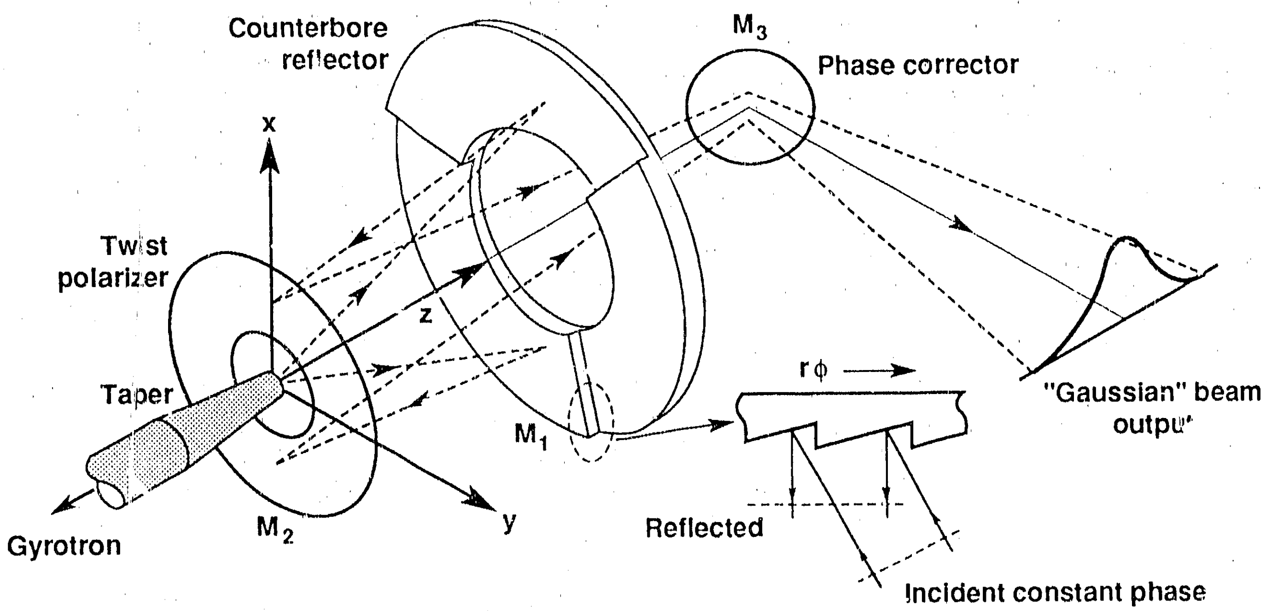


FIGURE 7. Drawing of the MAGICTRAC mode converter for whispering-gallery modes.

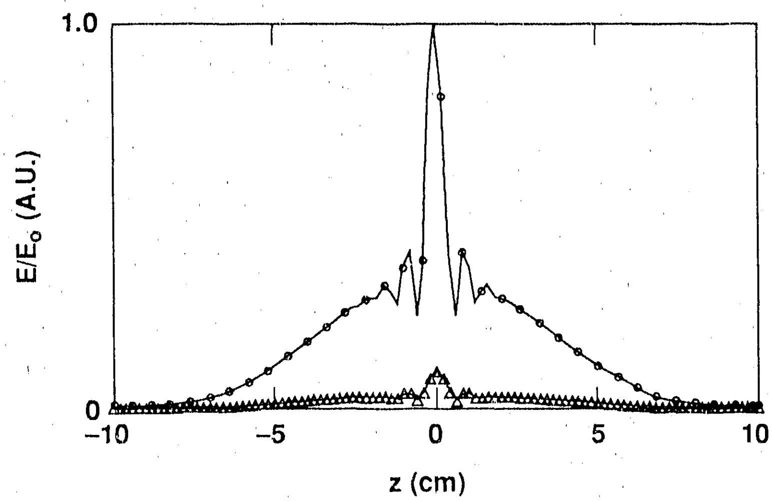


FIGURE 8. Aperture electric field profile incident upon the phase correcting optic ($M_3$) of MAGICTRAC. The triangle data points show the cross-polarized component.

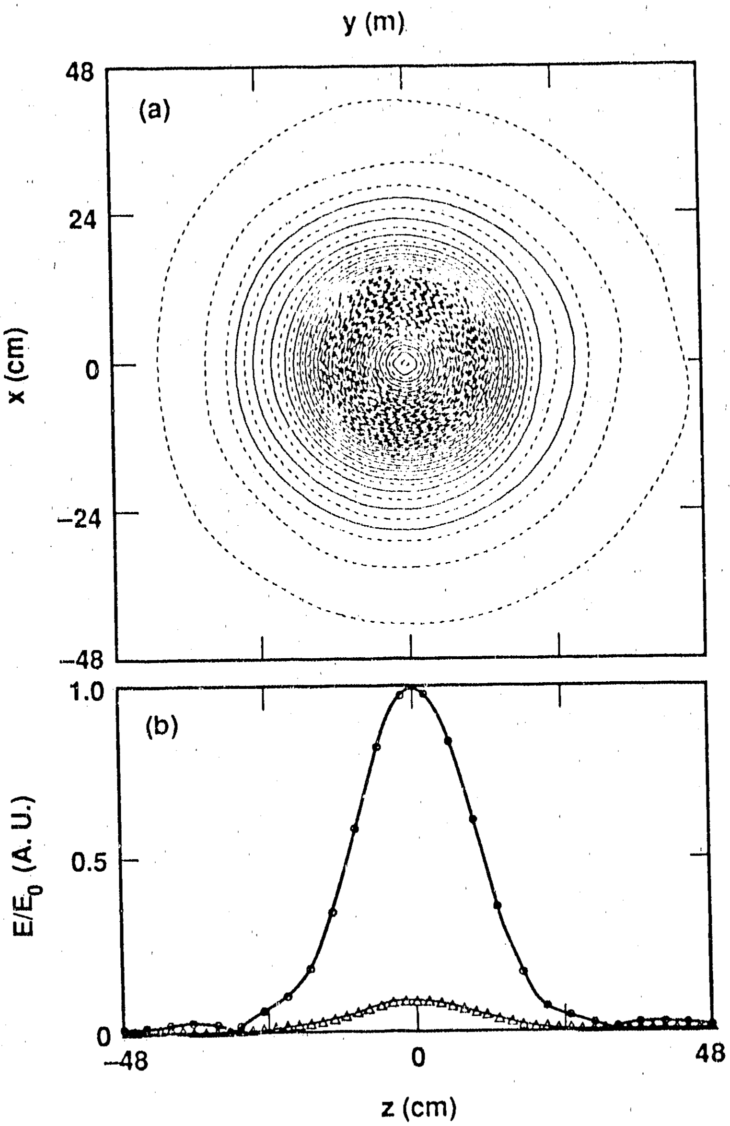


FIGURE 9. MAGICTRAC output beam electric field profile at 8 m from $M_3$. The triangle data points show the cross-polarized component.

# END

# DATE FILMED

10 / 23 / 90